REPORT DOCUMENTATION PAGE

Form Approved
OMB No. 0704-01-0188

PLEASE DO NOT RETURN YOUR FORM TO THE ABOVE ADDRESS.

1. REPORT DATE *(DD-MM-YYYY)*	2. REPORT TYPE	3. DATES COVERED *(From - To)*
28-06-2007	REPRINT	

4. TITLE AND SUBTITLE

Thermospheric Space Weather Modeling

5a. CONTRACT NUMBER

5b. GRANT NUMBER

5c. PROGRAM ELEMENT NUMBER
61102F

6. AUTHORS
Frank A. Marcos
William J. Burke
Shu T. Lai.

5d. PROJECT NUMBER
5021

5e. TASK NUMBER
RS

5f. WORK UNIT NUMBER
A1

7. PERFORMING ORGANIZATION NAME(S) AND ADDRESS(ES)

Air Force Research Laboratory /VSBXT
29 Randolph Road
Hanscom AFB, MA 01731-3010

8. PERFORMING ORGANIZATION REPORT NUMBER
AFRL-VS-HA-TR-2007-1069

9. SPONSORING/MONITORING AGENCY NAME(S) AND ADDRESS(ES)

10. SPONSOR/MONITOR'S ACRONYM(S)
AFRL/VSBXT

11. SPONSOR/MONITOR'S REPORT NUMBER(S)

12. DISTRIBUTION/AVAILABILITY STATEMENT
Approved for Public Release; distribution unlimited.

13. SUPPLEMENTARY NOTES
Reprinted from .Proceedings, 38th AIAA Plasmadynamics and Lasers Conference, 25-28 June, 2007, Miami, FL.

14. ABSTRACT

We review impacts of satellite drag and describe past, current and future capabilities designed to meet evolving operational requirements. Historically, thermospheric research has been data starved. Thus, from the early space age to the end of the 20 th century little progress was made in satellite-drag modeling. This condition improved greatly with the development of empirical assimilative models and recent availability of comprehensive drag measurements. With the new Jacchia-Bowman 2006 model the status of empirical modeling improved significantly. It builds on the expanded satellite drag database and incorporates improved estimates of solar flux changes as well as semiannual and local time variations of the thermosphere. However, magnetic storm representations of Jacchia-Bowman 2006 are similar to those used in other current models. Satellite-borne accelerometers and optical sensors now provide complementary spatial and temporal capabilities that permit monitoring of the thermosphere over a wide range of altitudes under most solar and geomagnetic conditions. Long-standing shortfalls during periods of high geomagnetic activity are now being attacked with these data and through new analyses of solar wind and IMF measurements, correlations with magnetosphere-based magnetic indices and emerging theoretical tools. These advances in understanding thermospheric coupling during magnetic storms will be incorporated into empirical model upgrades. The analyses of new data sets joined with on-going research on physical thermosphere-ionosphere-magnetosphere coupling processes support the pursuit of our ultimate goal, an assimilative and predictive operational model of thermospheric neutral densities.

15. SUBJECT TERMS

Satellite drag Thermospheric densities Assimilation models

16. SECURITY CLASSIFICATION OF:			17. LIMITATION OF ABSTRACT	18. NUMBER OF PAGES	19a. NAME OF RESPONSIBLE PERSON
a. REPORT	b. ABSTRACT	c. THIS PAGE			Frank A. Marcos
UNCL	UNCL	UNCL			19B. TELEPHONE NUMBER *(Include area code)*

38th AIAA Plasmadynamics and Lasers Conference
 In conjunction with the
 16th
25 - 28 June 2007, Miami, FL

AIAA 2007-4527

AFRL-VS-HA-TR-2007-1069

Thermospheric Space Weather Modeling

Frank A. Marcos[1], William J. Burke[2], and Shu T. Lai[3]
Space Vehicles Directorate, Air Force Research Laboratory, Hanscom AFB, MA 01731

We review impacts of satellite drag and describe past, current and future capabilities designed to meet evolving operational requirements. Historically, thermospheric research has been data starved. Thus, from the early space age to the end of the 20th century little progress was made in satellite-drag modeling. This condition improved greatly with the development of empirical assimilative models and recent availability of comprehensive drag measurements. The resurgence in orbital drag analyses to specify thermospheric densities has been particularly useful for addressing input requirements of assimilation models as well as their development and validation. With the new Jacchia-Bowman 2006 model the status of empirical modeling improved significantly. It builds on the expanded satellite drag database and incorporates improved estimates of solar flux changes as well as semiannual and local time variations of the thermosphere. However, magnetic storm representations of Jacchia-Bowman 2006 are similar to those used in other current models. Satellite-borne accelerometers and optical sensors now provide complementary spatial and temporal capabilities that permit monitoring the thermosphere over a wide range of altitudes under most solar and geomagnetic conditions. Long-standing shortfalls during periods of high geomagnetic activity are now being attacked with these data and through new analyses of solar wind and IMF measurements, correlations with magnetosphere-based magnetic indices and emerging theoretical tools. These advances in understanding thermospheric coupling during magnetic storms will be incorporated into empirical model upgrades. The analyses of new data sets joined with on-going research on physical thermosphere-ionosphere-magnetosphere coupling processes support the pursuit of our ultimate goal, an assimilative and predictive operational model of thermospheric neutral densities.

Nomenclature

A	=	satellite cross-sectional area
a_D	=	orbital drag acceleration
B	=	ballistic coefficient
C_D	=	satellite drag coefficient
Dst	=	disturbance storm time index
EUV	=	extreme ultraviolet
E_{vs}	=	Volland-Stern electric field
F10.7	=	index of solar 10.7cm flux
FUV	=	far ultraviolet
g	=	gravity
kp	=	magnetic activity index describing variation in the geomagnetic field
L_1	=	first Lagrange point
M	=	satellite mass
m	=	mean molecular mass
R	=	gas constant
ρ	=	atmospheric density
$<\rho_T>$	=	average thermospheric density
T	=	atmospheric temperature
V	=	satellite velocity relative to the ambient gas

[1] Senior physicist, Space Weather Center of Excellence, Mail Stop: VSBXT; Member AIAA.
[2] Emeritus, Space Weather Center of Excellence, Mail Stop: VSBXI.
[3] Senior physicist, Space Weather Center of Excellence, Mail Stop: VSBXT; Associate Fellow AIAA.

I. Introduction

Aerodynamic drag continues to be the largest uncertainty in determining orbits of satellites operating in Earth's upper atmosphere below about 600 km. Drag errors impact many aerospace missions including precision satellite orbit determination and prediction, collision avoidance warnings, reentry prediction, lifetime estimates and attitude dynamics. Orbital drag accelerations (a_D) for a satellite in the Earth's atmosphere are related to neutral density (ρ) by:

$$a_D = - \frac{1}{2} (C_D A/M) \rho V^2 \quad (1)$$

where C_D, A, M and V are respectively the satellite drag coefficient, cross-sectional area, mass, and velocity relative to the ambient gas. Uncertainties about neutral densities are the major source of drag errors and are the subject of the remainder of the paper. Assuming A/M is known, the other terms in order of importance are generally the satellite's drag coefficient, C_D, and the neutral wind. Drag coefficient errors are typically assumed to be ~10%. The neutral wind enters the drag equation through the total atmospheric velocity relative to the satellite. Thus, winds of 200 m/sec contribute about 5% to the total drag. However, during large geomagnetic storms, winds of ~1 km/sec have been observed at high latitudes.

This paper focuses on thermospheric density variations above 90 km, where temperature rises drastically to ~600 - 2000 K. The density and hence drag in this region is driven mainly by two solar influences: directly by EUV radiation (solar photons) and indirectly by the solar wind (corpuscular radiation). Solar EUV is the main mechanism for heating the Earth's thermosphere and creating the ionosphere. On average EUV radiation, at wavelengths < 200 nm, accounts for about 75 - 80% of the energy input to the thermosphere, and thereby determines its basic structure. It is deposited mainly at low to mid latitudes, in the sub solar region. This heating creates a pressure bulge that drives winds to transport heat away from the hot dayside toward the Earth's cold nightside. Temperatures on the dayside are typically 30% higher than those on the nightside. Solar EUV fluxes originate in the chromosphere, chromosphere-corona transition region and corona. In contrast to visible radiation, EUV emissions are highly variable, with chromsopheric emissions changing by a factor of 2 or more and coronal emissions varying by a factor of 50-150 over the solar cycle.

Geomagnetic activity is low about 90% of the time and on average accounts for about 20% of the heating of the thermosphere. During geomagnetic storms, the disturbed solar wind compresses the Earth's magnetosphere. Intense electric fields in the high-latitude ionosphere drive rapid plasma convection that couple via collisions with neutral winds. At the same time, the auroral oval expands and energetic particles precipitating into the lower thermosphere enhance ionospheric conductivities. Intense field-aligned currents couple the auroral ionosphere with the magnetosphere extracting electromagnetic energy (Poynting flux) that heats both the ionized and neutral gases. The resultant heating expands the neutral atmosphere; changes local neutral compositions, generates traveling gravity waves and excites strong winds[1]. The rate of electromagnetic energy input at high latitudes energy can rise to more than ten times greater than that of the global EUV.

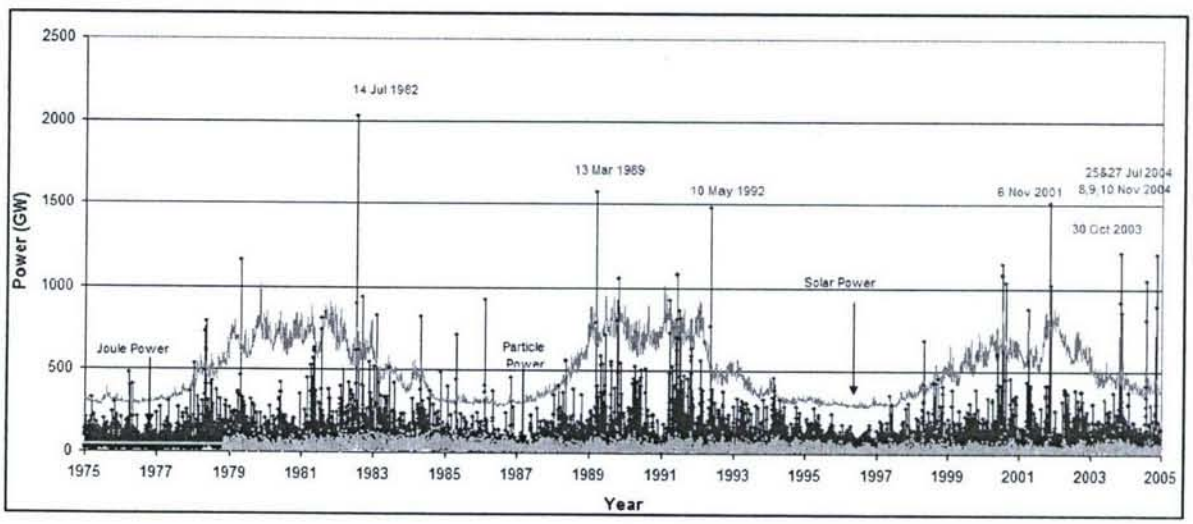

Figure 1. Profiles of power inputs at the top of the atmosphere from 1975 through 2004. Data are for geomagnetic activity (blue), solar EUV (solid gray, top curve) and particles (dotted gray, bottom).

Knipp[2] calculated energy inputs from solar EUV, "Joule" heating and particle deposition for the period 1975 to 2005 (Figure 1). This figure illustrates that the thermosphere is a dynamic region mainly dependent on the relative heating due to solar EUV radiation at low latitudes and to auroral processes, associated with the solar wind, at high latitudes. EUV

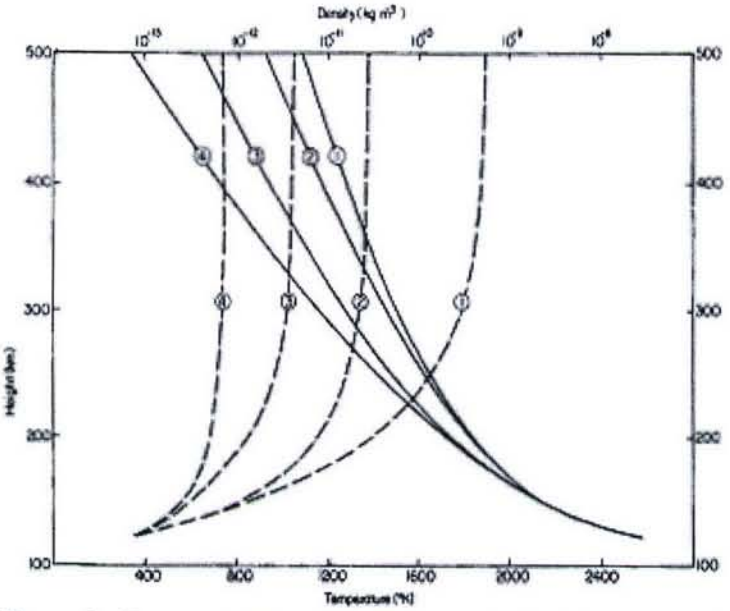

Figure 2. Representative empirical model data showing vertical distribution of density and temperature as a function of solar activity. Curves are for high solar activity at noon (1) and midnight (2) and for low solar activity at noon (3) and midnight (4). Over the solar cycle the exospheric temperature varies by a factor of about 3 while the density increases by more than an order of magnitude at altitudes above 400 km.

sources exhibit solar cycle, solar rotation and day-to-day variabilities; storm effects are episodic. A generally less significant energy source, waves propagating up from the lower atmosphere, further modulates the thermosphere. The density of the air particles consequently is sensitive to solar activity, season, longitude, latitude, local time and magnetic storm conditions. These unpredicted and irregular changes in the atmospheric density are experienced by satellites in low-Earth orbit as described by Eq. 1. The ranges of thermospheric temperature and density variations are illustrated in Figure 2. The neutral density decreases exponentially with altitude. Assuming diffusive equilibrium (not valid during geomagnetic storms), the density depends on the scale height (RT/mg) where R is the gas constant, T is the temperature (dependent on solar cycle and geomagnetic activity), m is mean molecular mass and g is the acceleration due to gravity. Below about 110 km, turbulence mixes the atmospheric constituents. At higher altitudes the different species are separated gravitationally such that the main thermospheric constituent is generally atomic oxygen above about 200 and ~600 km. Helium densities compete with atomic oxygen above about 600 km during low solar flux conditions. For comparison, we note that the number densities of atmospheric neutrals near the height of the F2 peak are more than order of magnitude larger than those of free electrons.

Figure 3 outlines procedures used to predict satellite orbits. Atmospheric densities calculated from a model are applied in an orbit propagator to calculate future positions. To update any existing orbit, observations are first collected. Air Force Space Command (AFSPC) uses the Space Surveillance Network (SSN) to provide the required observations. This network uses radar sensors for near-Earth tracking (< 6,000 km altitude). Over a full geomagnetically quiet day, orbital drag affects a satellite's along-track position by ~800 km at 200 km altitude and ~8 km at 400 km. Under disturbed geomagnetic conditions these errors can more than double. Thus, accurate density knowledge is critical for collision avoidance calculations for the International Space Station and other high-value assets. Satellite lifetimes strongly depend on solar activity as well as altitude (Figure 4). This chart assumes that the same solar flux is experienced throughout its lifetime.

Under the illustrated conditions the lifetime of a satellite initially at 400 km is reduced from about 4 years at solar minimum to about a half year under solar maximum conditions[3]. Atmospheric density uncertainties also degrade the capability to determine the time of a satellite's reentry. During quiet geomagnetic conditions, 24 hour and 2 hour predictions are found to have average errors of 1 hr 46 min and 14 min. respectively[4]. For a typical satellite, 14 minutes corresponds to a distance of >6500 km. During geomagnetically active times, these errors increased to 3 hr and 42 min for 24 hour predictions and to 36 minutes for the 2 hour predictions. Therefore it is not possible to accurately predict the location of the reentry. Better knowledge of space weather and the responses of Earth's upper atmosphere are required to make

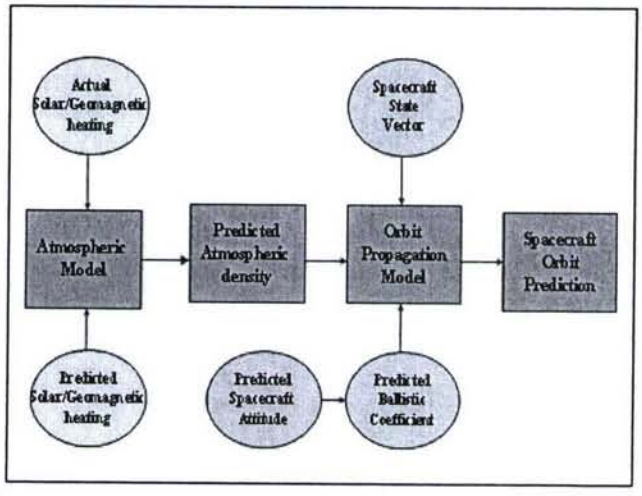

Figure 3. Satellite orbital prediction technique block diagram. Atmospheric density predictions are needed to calculate future positions of the spacecraft.

meaningful progress on low Earth orbit determination issues.

Progress in understanding the satellite drag environment can be conveniently described in two in two steps: intra- and post-20th century. Section II describes development of models based on limited datasets between the dawn of the space age and the century's end. Section III highlights some selected areas of research that exploit new databases and modeling techniques now becoming available. Section IV summarizes progress in Air Force operational satellite drag modeling capabilities.

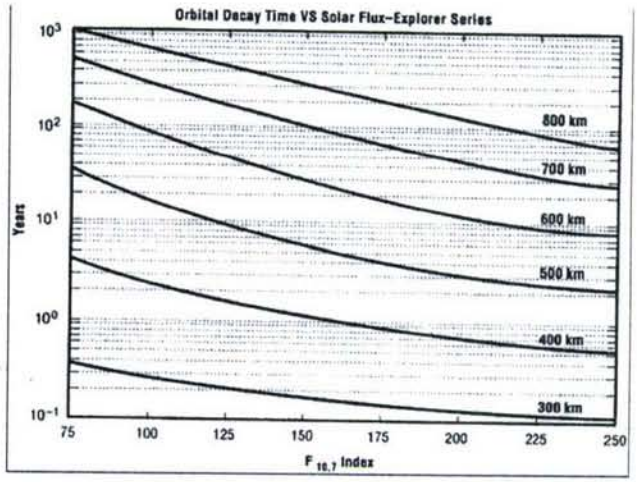

Figure 4. Satellite Lifetime vs Altitude and Solar Flux.

II. Model Development in the Late 20th Century

Neutral density variations in the thermosphere due to diurnal, seasonal, semiannual, solar activity and geomagnetic disturbances were first incorporated into the Jacchia 1964 (Ref 5) model that laid the foundation for empirical models still used today. The model is built on analytical representations of temperature height profiles as functions of latitude, local time, day of year, solar activity index (F10.7) and geomagnetic indices (Kp or ap). A persistent problem for modelers has been the lack of direct solar EUV and auroral heating (particles and electric fields) data. In the absence of the needed solar observations, all empirical models used the F10.7 solar radio flux as a surrogate for solar EUV heating and the 3-hourly Kp index to represent the level of geomagnetic activity. The solar flux term incorporates two components, daily and time-averaged values. Height profiles of the major constituents are calculated as a function of exospheric temperature assuming diffusive equilibrium with fixed boundary conditions at 120 km. An exponential form for the temperature distribution that closely approximates theoretical profiles allows the hydrostatic equation to be integrated explicitly to estimate density as a function of height. Model inputs are position, time and geophysical indices for solar and auroral heating. Outputs are temperature, composition and density. Semiannual variations, observed to change from year to year via unknown mechanisms, are represented by climatological averages. The Jacchia 1970[8] (J70) model, based on drag measurements from ~16 satellites in the 1960's, refined the relationships between solar drivers and density, improved the semiannual variation climatology and moved the lower boundary to 90 km, using constant temperature and constituent densities. J70 continues to be the basis for operational density models at Air Force Space Command. The NASA MET[9] (Marshall Engineering Thermosphere), developed at the NASA Marshall Space Flight Center, approximates J70, but uses a 162 rather than 81 day averaged solar flux to provide total mass density, temperature and composition It is used operationally by NASA to estimate satellite lifetimes, orbit insertion, orbit determination and tracking, attitude dynamics and reentry prediction. Mass Spectrometer and Incoherent Scatter (MSIS) models[6] developed between 1977 and 1990 utilize atmospheric composition data from instrumented satellites and temperatures from ground-based radars. Although published in 2002, the NRLMSISE-00 model[7] is included in this suite since it is based on in-situ and orbital databases acquired prior to 2000.

Figure 5 summarizes the problem that confronts scientific and operational users of neutral density models[10]. One-sigma standard deviations for versions of the Jacchia and MSIS models produced between 1964 and 1990 remained near 15%. A notional depiction of the amount of data available for model development is represented in Figure 5 as a solid line. It shows that progress in modeling was essentially stagnant even as databases increased significantly. New data sets advanced understanding the morphology of drag variations but did not yield commensurate improvements in quantitative modeling[9]. The inadequate proxies used by empirical drag models are the major sources of drag uncertainties. The MSIS models provide superior descriptions of atmospheric composition. However, the versions of the J70 model were used operationally by a number of organizations including AF Space Command and NASA MSFC

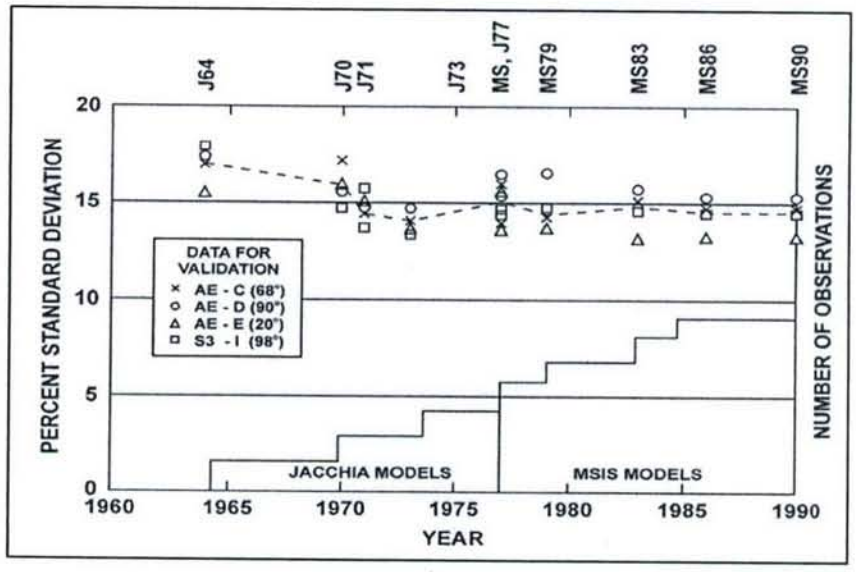

Figure 5. Accuracy of satellite drag models vs time. The Jacchia and MSIS series of models are labeled by a J or MS respectively and a year at the top of the curve. The solid line at the bottom of the curve is a notional indicator of the amount of data used in development of each model.

since it was available before the advent of the MSIS models, used less computer time and was equivalent in satellite drag accuracy.

Ideally, physical models of solar behavior and solar terrestrial interactions should form the basis of upper atmospheric density forecasts. Thermosphere General Circulation Models solve the neutral gas equations of continuity, momentum, energy and mean molecular mass. Solution of the related differential equations provides global distribution of the mass density temperature and three components of neutral winds. These complex physical models allowed great progress, revealing the physics of thermospheric variations via coupling to the ionosphere and magnetosphere. Further, they have accuracies about same as empirical models[11,12,13]. However, the observational solar data sets needed to achieve the potential accuracy of these models are not presently available. Consequently the satellite drag community continues to rely on simpler empirical models driven by proxy indicators of solar heating. These empirical models remain the focus of this paper.

A significant advance in modeling was achieved by demonstrating that neutral density models can be corrected in near real time with satellite drag data obtained via ground-based tracking[14]. This approach used "calibration" satellites with known area to mass ratios to extract corrected neutral density values. The black line in Figure 6 shows operational tracking data for the LDEF (Long Duration Exposure Facility) satellite. This satellite was selected because of its nearly constant area-to-mass ratio. The orbit determination process best fit the satellite tracking observations in a least squares sense by solving for a ballistic coefficient (C_DA/M) using the density predicted by the J70 model. If the model density was low (high), then the ballistic coefficient was correspondingly increased (decreased). However, assuming constant C_DA/M, the operational corrections to the ballistic coefficient (B) should be interpreted as corrections in model densities over the fit span. For example, a 5%

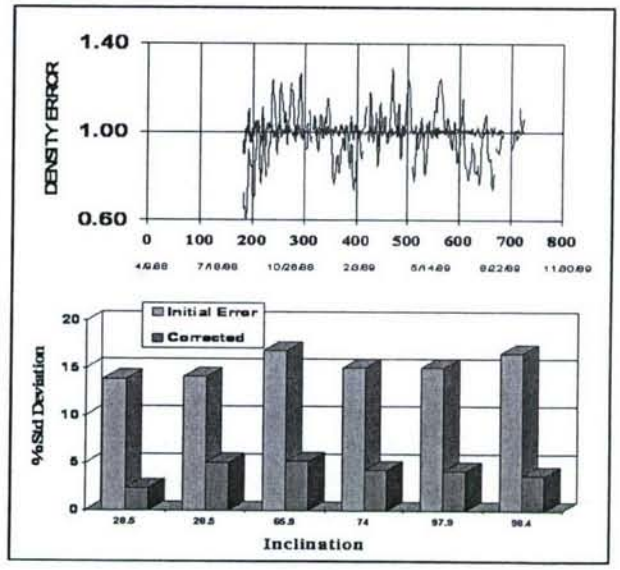

Figure 6. Model error reduction with data assimilation. Use of time dependent model corrections to an empirical model dramatically reduced the ballistic coefficients from ~15% (blue) to ~5% (green).

overestimate in B corresponds to a 5% density underestimate by J70. These corrections to the operational density model were then used to modify the heat input to J70 and permitted the calculation of corrected global neutral density fields. The model correction applied to LDEF July 1988 - December 1989 reduced ballistic-coefficient variations to about 2.3%. Use of these new time-dependent global density fields reduced orbit-determination errors for satellites in different orbits from about 15% to 5% (bottom half of Figure 6). "Atmospheric calibration" technique circumvents errors in model inputs and inadequacies to improve the precision of orbit determination. Thus, at the end of the 20th century, a new approach to reduce density model errors was introduced.

Year	Experiment	Data	Lifetime	Agency
1981	DE-2	Composition	18 Mos.	NASA
1982	SETA-2	Density	8 Mos.	AFRL
1983	SETA-3	Density	8 Mos.	AFRL
1985	S85-1	Density	3 Mos.	AFRL
1988	San Marco	Density	8 Mos.	NASA
2000	CHAMP	Density	7+ Yrs.	GFZ Potsdam
2000	TIMED GUVI	Composition	6+ Yrs.	NASA/APL/Aerospace
2002	GRACE	Density	5+ Yrs.	CSR, Texas
2003	SSUSI	Composition	4+ Yrs.	DMSP/APL/NRL
2003	Orbital Drag	Density	40 Yrs.	AFRL/AFSPC/NRL

Figure 7. Satellite density measurements before and after 2000.

III. Satellite Drag Progress in the 21st Century

A. Overview of New Measurements

Historically, thermospheric density measurements have been sparse. New measurements are providing an abundance of data as functions of altitude, latitude, local time day of year and solar and geomagnetic conditions. Figure 7 compares the availability of thermospheric measurements in the 20-year period 1980 - 1999 with that of the last six years. The new data sources include the CHAMP[15] (CHAllenging Minisatellite Payload) and GRACE[16] (GRAvity and Climate Experiment) accelerometers, the TIMED (Thermosphere Ionosphere Mesosphere Energetics and Dynamics) GUVI [17] (Global Ultra Violet Imager) and SEE[18] (Solar Extreme Ultraviolet Experiment) instruments, operational DMSP SSUSI[19] (Special Sensor Ultraviolet Spectrographic Imager) density remote sensors and extensive long-term orbital drag measurements[20]. We are currently in a "Golden Age of Satellite Drag." New programs routinely measure drag and density globally. New solar and geomagnetic indices are being developed to improve empirical and physical inputs needed to implement sophisticated assimilation techniques. These programs are directed toward dramatically reducing satellite drag errors and increasing forecast times to meet stringent present and evolving operational requirements. Selected aspects of these new capabilities being currently exploited in Air Force modeling are described below.

B. Expanded Orbital Drag Databases

Orbital decay measurements provided the first realistic upper atmosphere density data. They are the basis for the J70 model still utilized operationally by most satellite drag communities including Air Force Space Command and NASA MSFC. This measurement technique has been greatly improved to develop the comprehensive, high-resolution historical database[21], extending from 1966 to 2003, needed to evaluate and improve empirical models. Accurate daily density values are obtained from drag analysis of low perigee, high elliptical orbit satellites. Daily temperature values were computed using a procedure in which tracking observations are fit using a special orbit-perturbations method[22]. The initial database used over two dozen satellites to attain unprecedented coverage under a wide range of solar/geomagnetic conditions that produced neutral densities with one-day resolution[22] and an accuracy of about +/- 4%. Figure 8 shows

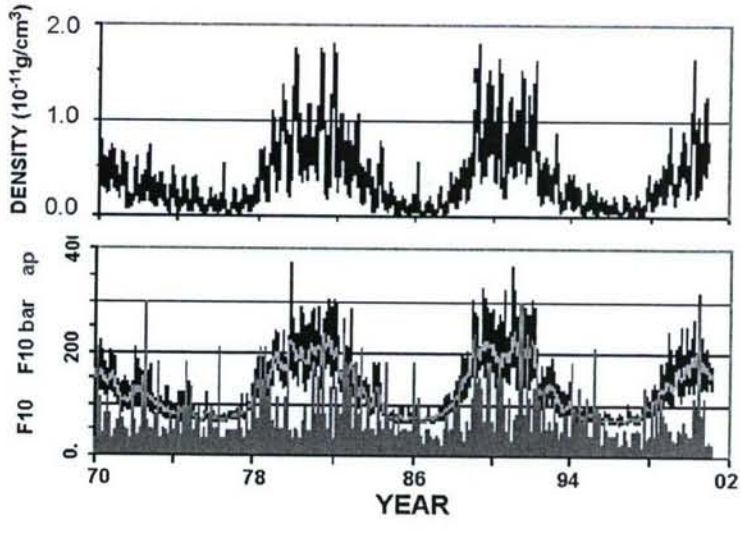

Figure 8. Density as function of day of year from 1970 to 2001 at 400 km (top); solar flux (F10.7) and the level of geomagnetic activity (ap). (bottom).

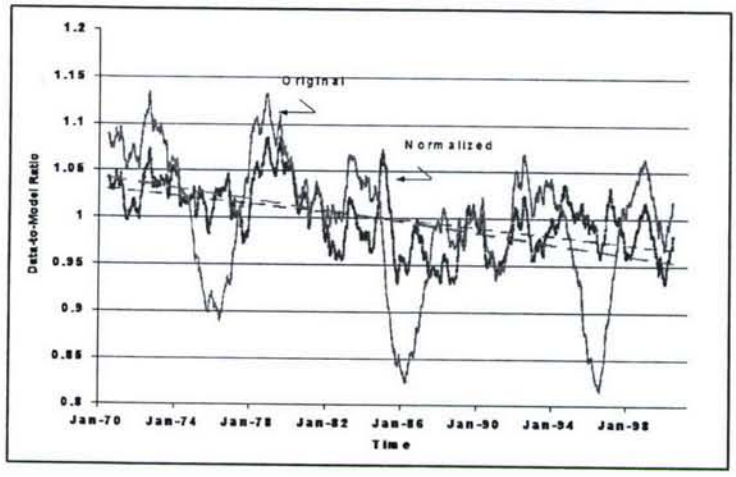

Figure 9. Thermospheric cooling. Comparison of density data to model results vs time obtained two ways: (a) from unnormalized (green) and (b) normalized (red) data. Dashed lines are linear regression fits.

densities obtained from a single satellite at 400 km latitude (top frame) over solar cycles 20 to 23 (1970 – 2001). Traces of the F10.7 and ap indices plotted in the bottom panel of Figure 8 represent prevailing solar and geophysical conditions.

The detection of unmodeled thermospheric variations[23,24,25] associated with increased greenhouse gases is an additional result of long-term database analyses. Similar effects were also uncovered in the analyses of ionospheric F2 layer heights[19]. First-principle model simulations[2] predicted that a doubling of CO_2 would cause thermospheric density to decrease by about 40% at 400 km near solar minimum and 18% near solar maximum. Data shown in Figure 9[25] indicate a density decline of about 5% over 30 years (average solar flux of 128 units) corresponding to a CO_2 increase of 12.5%. If the density decline is linearly related to CO_2 concentration, then these results appear to be in close agreement with theory. Consequent to thermospheric cooling the lifetimes of space objects will increase as will the probability of collisions. These studies illustrate the continuing applications and requirements for improved satellite drag models over all time scales.

C. Assimilative Operational Models

The Air Force High Accuracy Satellite Drag Model (HASDM)[27,28,29] optimizes the concept of "atmospheric calibration[14]" by simultaneously tracking ~75 calibration satellites. Observations and statistical uncertainties are directly applied to solving for satellite state vectors. Density is determined using a single weighted differential estimation process that generates average corrections to J70 temperatures every three hours. Globally corrected density fields are then determined with the corrected temperatures. The concept was tested in 2001 and operational implementation began in September 2004. HASDM typically reduces satellite drag errors from about 15% to 8% overall (4% for the calibration satellites) and provides a one-day forecast capability. Thus, it cuts the persistent deficiency in satellite drag operations by about a factor of two.

D. New Orbital Drag Model

The new Jacchia-Bowman (JB2006)[30] model exploits the availability of new historic satellite drag datasets.. This model is based on the Jacchia model heritage. The major differences are in solar flux inputs, the semiannual formulation and local time variations. These additions were developed and tested against large satellite-drag databases. Approximately 120,000 orbital drag data points were used in developing the new model's equations. The satellites had perigee altitudes ranging from 175 km to 1100 km and covered the period 1978 through 2004. Solar indices have three components: EUV measurements in the 250-300 nm range from the SOHO satellite, FUV MgII data (from Solar Backscatter Ultraviolet spectrographs on Nimbus satellites) and $F_{10.7}$. The semiannual variation changes with height and time, and depends on solar flux rather than the climatological averages of J70. Local time corrections were determined as a function of altitude, latitude

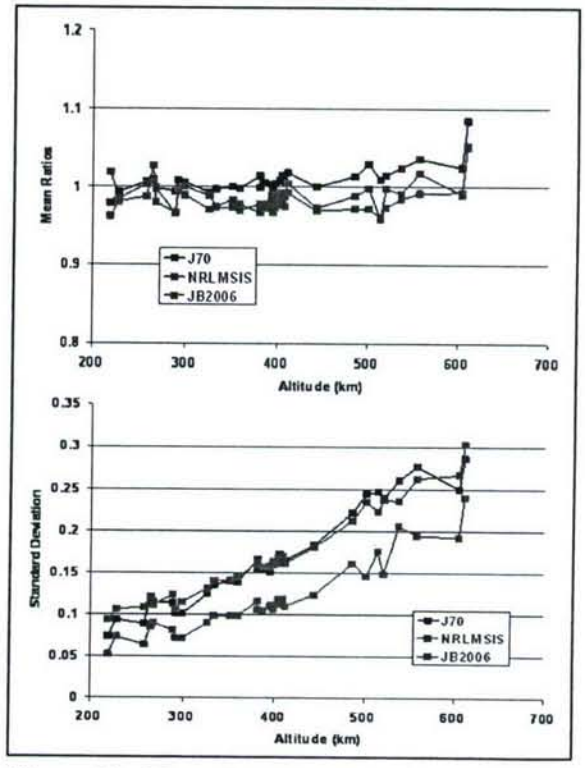

Figure 10. Mean data-to-model ratios (top) and standard deviations (bottom) for JB2006, J70, and NRLMSIS models vs altitude.

and solar flux. JB2006 is currently applicable for the period 1997 through 2004, when the required SOHO solar indices are available. A limitation of the model is that the formulation for geomagnetic storm periods is unchanged from J70.

An evaluation of JB2006 with independent orbital drag data shown in Figure 10 indicate that mean values are similar to those of the J70 (and MET, not shown since results were essentially the same as those from J70) and NRLMSISE models (top frame), but that the standard deviations are lower at all altitudes[31] (bottom frame). Overall standard deviations are reduced by about 5%. This is the first significant error reduction in (non-assimilative) empirical models.

A planned upgrade (designated JB2008) will advance JB2006 in five areas: (1) use high-resolution, full-spectrum solar EUV inputs from the TIMED/SEE sensor: The TIMED Solar EUV Experiment (SEE) provides the first comprehensive solar EUV data since the Atmosphere Explorer –E measurements during 1975-1981 , (2) develop new equations for geomagnetic storm periods, (3) model the localized high latitude density enhancements seen in CHAMP accelerometer data [32,33], (4) upgrade the formulations semiannual variations, and (5) improve drag coefficients for satellite reentry studies. The following section describes planned improvements applicable to geomagnetic storm periods.

E. Geomagnetic Storm Analyses

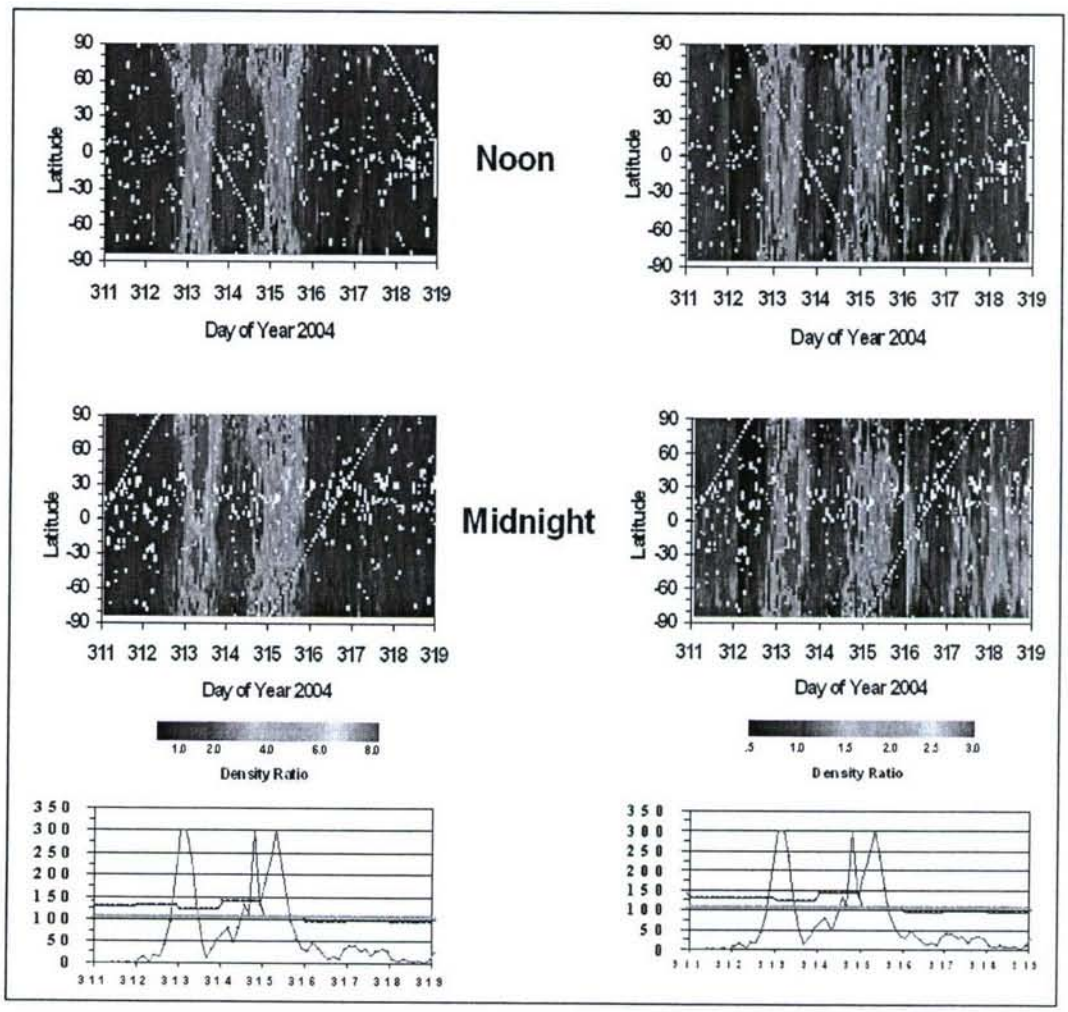

Figure 11. GRACE noon densities (top left) and midnight densities (middle left) in latitude-day of year coordinates normalized to day 311 values; corresponding NRLMSISE model values (top and middle right); bottom curves are solar-geomagnetic conditions.

Serious shortcomings of present empirical models are most evident during large magnetic storms when complex thermospheric responses become difficult to capture. Initial responses to storm electrodynamics include Joule and frictional heating that raise thermospheric temperatures as well as enhanced ion drag that drives high-speed neutral winds at high latitudes. The stormtime heat sources induce divergent wind surges that propagate from

both polar regions toward lower latitudes and beyond into the opposite hemispheres. Vertical components accompanying the divergent wind fields propel material across pressure surfaces, and carry molecule-rich gas to higher levels. Consequent composition "bulges" of increased mean molecular mass are then transported by storm-induced and background winds. Numerical simulations suggest that the prevailing summer-to-winter circulation near solstices transports the nitrogen-rich gas to mid and low latitudes in the summer hemisphere over a day or two following storms[34]. These composition responses are responsible for positive (increased atomic oxygen) and negative (increased molecular nitrogen) ionospheric storms.

The recent availability of accelerometer measurements from the CHAMP and GRACE satellites facilitates new attempts to address stormtime shortcomings. CHAMP data indicate that during the superstorms of October and November 2003 models underestimated density responses by as much as a factor of two[35, 36]. Data from the superstorm of 8 - 10 November 2004 are shown in Figure 11 to illustrate the extremes of thermospheric variability[37]. Magnetic activity maximized during days 312 – 315, with ap reaching 300 in two consecutive 3-hr intervals on day 313, at the end of day 314 and in the middle of day 315. To facilitate interpretation of the variability, densities in 2-degree latitude bins are normalized to the quiet conditions of day 311. The relative variations are large, reaching values >5. GRACE measurements are shown in left panel of Figure 11. The ratios of measured density to NRLMSISE-00 predictions, shown in the right panel of Figure 11, indicate that the model underestimated responses by as much as a factor of 3.

Simultaneous measurements from ion drift meters and magnetometers on DMSP satellites are now being used to estimate net Poynting fluxes into the ionosphere and stormtime thermospheric heat budgets. During the main phase of the storm of April 2000 four DMSP satellites detected large quantities of energy being deposited into the auroral ionosphere but ground measurements no commensurate magnetic perturbations[38]. This behavior is a late main-phase feature of most large (Dst $\leq$ -200 nT) storms. Models that rely solely on their measurements would significantly underestimate thermospheric energy budgets during such storms. Figure 12 summarizes results between a comparison of GRACE measurements with magnetic and electro-dynamic parameters acquired during the magnetic storm of November 8 – 10, 2004[39]. Thermospheric mass densities ρ_T derived from the accelerometers on the GRACE satellites are shown with superposed orbit-averaged densities $< \rho_T >$ (blue) and with variations of the indices Dst and E_{vs}. The red line in the top frame show values of Dst. E_{VS} is the electric field in the inner magnetosphere estimated with a modified Volland-Stern model. Its variations, represented by the red trace in the bottom panel, were determined from solar wind and interplanetary magnetic field data acquired by the Advanced Composition Explorer (ACE). From the beginning of the main phase through the early recovery phase (~08:00 UT, 8 November) Dst and ρ_T were highly correlated. After this time through the first half of 9 November, the thermosphere relaxed at a faster rate than Dst. Stormtime activations of 9 - 10 November proceeded in two stages. In the second and more disturbed period, thermospheric responses seem to precede Dst by about an hour. Again the thermosphere relaxed more quickly than Dst during recovery. Variations of E_{vs} and $< \rho_T >$were quite similar in form throughout the entire storm. Structures in E_{vs} traces consistently preceded those of $< \rho_T >$ by several hours. With a constant lead time of 4 hours the correlation between the two quantities is ~0.87. This suggests a new basis for gaining 4-hour predictions of stormtime disturbances using standard data measured by ACE near the L_1 point. These observational results form the basis of a new research effort to improve stormtime predictions of the new JB2008 model.

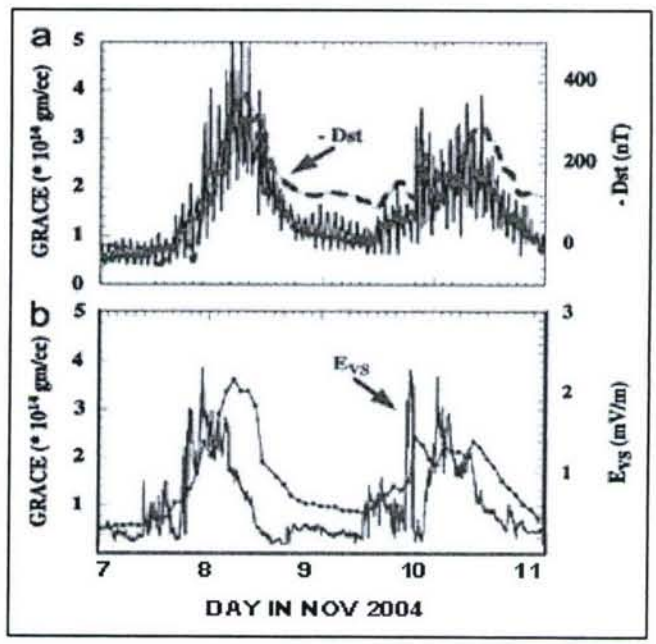

Figure 12. Top: GRACE measurements during the Nov 04 storm period with superposed orbit-averaged densities (blue) and with variations of the indices Dst (red) index. Bottom: Orbit averaged GRACE densities (blue) and Evs (red). Evs is the electric field in the inner magnetosphere determined from the Volland -Stern model (red), derivable from ACE (Advanced Composition Explorer) satellite data at the L1 point.

Returning to the top panel of Figure 12, we direct the reader's attention to the presence of large positive and negative spikes in the instantaneous measurements of "ρ_T". They occur at magnetic high latitudes and are unpredicted by models. Comparisons with near simultaneous ion drift measurements from DMSP satellites suggest that

rapidly varying accelerometer measurements reflect encounters with strong (≥1 km/s) head and tail winds in the thermosphere driven by plasma convecting in the anti-sunward direction across the polar caps.

F. Thermospheric Winds and Satellite Drag

As equation (1) indicates, although neutral winds contribute to satellite drag their contribution to error budgets is generally small, ~5% for 200 m/s^{-1} winds. Empirical models of winds have been developed but have not been incorporated into drag models. If wind contributions were systematic, they could be absorbed into calculations that use density and drag interchangeably. However, especially at high latitudes, winds depend on Universal Time, local time, season, IMF orientations and episodic geomagnetic activity. The unmodeled wind effects associated with geomagnetic activity can introduce more significant drag errors. At high latitudes, energy and momentum sources associated with magnetosphere-ionosphere coupling strongly affect the dynamics of the thermosphere. Ion and electron precipitation create and maintain ionospheric plasma in the absence of solar EUV. Auroral and polar-cap electric fields convect plasma across the magnetic field, generally at finite velocities in the rest frames of thermospheric neutrals. During magnetic storms ion convection across the polar cap collisionally drags neutrals to generate winds with speeds that can exceed 1 kms^{-1} [39] at F layer heights introducing errors of ~25% or more in local drag estimates. Present day assimilative ionospheric models obtain composition from one empirical model[9] and winds from another[40]. The time is fast approaching when assimilative ionospheric and thermospheric models will be applied systematically to model and predict satellite drag.

G. New Neutral Density Multi-University Initiative (MURI)

A new 3-year MURI has been awarded to a team headed by the University of Colorado, with work scheduled to begin in FY08. This research will develop the physics and chemistry concepts required to accurately and reliably specify and forecast thermospheric neutral density to support both empirical and physical modeling. The initiative is intended to conduct critical basic research toward a near-real-time, accurate operational capability to locate, track identify, and estimate future locations of satellites with high accuracy. Key research goals include: (1) improved understanding of the physics of solar and geomagnetic quiet times, (2) understanding of how solar events couple into atmospheric effects, (3) a model of high latitude energy and its impact on the atmosphere, (4) a better method to measure neutral density and winds on a global scale, (5) a method to simultaneously measure Joule heating and neutral density response, (6) an understanding of the spatial and temporal distribution of energy sources of the thermosphere, (7) an understanding of the predictive potential and relative importance of solar energy sources to the thermosphere, and a determination of the time from prediction or observation to a change in atmospheric density. (8) development of physics-based indices to replace the statistical indices now in use, (9) precise determine of satellite drag coefficients, (10) an understanding of the physics of drag in the 200-100 km region with an object going from free molecular flow to slip flow. With the additional underpinning of this effort, we anticipate significant future progress in satellite drag capability.

IV. Summary

Uncertainties in neutral density variations have been the major limiting factor for precise low-Earth orbit determination. The combined new data sets from orbital drag, satellite-borne accelerometers and remote sensors provide unprecedented capabilities for understanding thermospheric variability. Solar EUV heating is the major energy source for the thermosphere and is also the major source of day-to-day satellite drag errors. Data are revealing new areas of thermospheric sensitivity to solar EUV and FUV. These issues can now be addressed with new, accurate measurements of the solar spectrum. The dramatic, though less frequent, geomagnetic storm effects can now be analyzed with detail previously unavailable. Variations as functions of latitude, day of year and local time are being routinely measured with high resolution, allowing previously unachievable analyses. The satellite drag problem is being vigorously and fruitfully attacked on several fronts: a variety of comprehensive measurements, data assimilation or "calibration" schemes, solar and geomagnetic indices, and the new MURI effort. The culmination of these efforts will be steady, previously unattainable, progress in meeting evolving stringent requirements for operations in the satellite drag environment.

References

[1]R.G. Roble, "The Thermosphere", *The Upper Atmosphere and Magnetosphere*, National Academy of Sciences, Washington, DC, 1977.

[2]Knipp, D., "Long and Short Term Variations in Thermospheric Heating Sources", AAS 05-253, *AAS/AIAA Astrodynamics Specialist Conference*, South Lake Tahoe, CA 2005.

[3]Owens, J. K., W.W. Vaughan, K. O. Niehuss and J. Minow, "Space Weather, Earth's Neutral Upper Atmosphere (Thermosphere) and Spacecraft Orbital Lifetime/Dynamics", *IEEE Trans. Plasma Sci.*, Vol 28, Dec. 2000.

[4]de la Barre, C., Capt., "Space Control Operations-Meeting the Challenge", *Proceedings of the Atmospheric Neutral Density Specialist Conference*, Colorado Springs, CO, March 1988.

[5]Jacchia, L.G, "Static Diffusion Models of the Upper Atmosphere with Empirical Temperature Profiles", *SAO Special Report No. 170*, 1964.

[6]Jacchia, L. G., "Revised Static Models of the Thermosphere and Exosphere with Empirical Temperature Profiles", *SAO Special Report No. 313*, 1970.

[7]Owens, J. and Vaughan, W., "Semi-Empirical Thermospheric Modeling: The New NASA Marshall Engineering Thermosphere Model - Version 2.0 (MET-V2.0)", *35th COSPAR Scientific Assembly*, 2004, July 2004, Paris, France. p. 2708.

[8]A. E. Hedin, C. A. Reber,, G. P. Newton, N. W. Spencer, H. C. Brinton, H. G. Mayr, H. G., and W. E. Potter, "A Global Thermospheric Model Based on Mass Spectrometer and Incoherent Scatter Data: MSIS 2 Composition", *J. Geophys. Res.*, Vol. 82, 1977, p. 2148.

[9]Picone, J. M., A. E. Hedin, D. P. Drob, and A. C. Aiken, "NRLMSISE-00 Empirical Model of the Atmosphere: Statistical Comparisons and Scientific Issues", *J. Geophys. Res.*, 107, 2002, p. 1468.

[10]Marcos, F. A., "Accuracy of Atmospheric Drag Models at Low Satellite Altitudes", *Adv. Space Res.*, Vol. 10, (3), 1990, p. 417.

[11]R.G. Roble, E.C. Ridley, A.D. Richmond and R.E. Dickinson, "A Coupled Thermosphere Ionosphere General Circulation Model", *Geophys. Res. Lett.*, 15,1988, p. 1325.

[12]Fuller-Rowell, T.J. and D. Rees, "A Three-Dimensional, Time-Dependent, Global Model of the Thermosphere", *J. Atmos. Sci*, 37, 1980, p. 2545.

[13]Richmond, A. D., E.C. Ridley and R.G. Roble, "A Thermosphere/Ionosphere General Circulation Model With Coupled Electrodynamics", *Geophys. Res. Lett.*, 19, 1992, p. 601.

[14]Marcos, F.A., M. Kendra, J. Griffin, J. Bass, J. Liu and D. Larson, "Precision Low Earth Orbit Determination Using Atmospheric Density Calibration", *J. Astronaut. Sci.*, 46, 1998, p. 395.

[15]Bruinsma, S., D. Tamagnan and R. Biancale, "Atmospheric Densities Derived from CHAMP/STAR Accelerometer Observations", *Plan. Spa. Sci.*, 52, 2004, p. 297.

[16]Tapley, B.D., S. Bettadpur, M. Watkins and C. Reigber, "The Gravity Recovery and Climate Experiment: Mission Overview and Early Results", *Geophs. Res. Lett*, 31(9), 2004, LO9607, doi:10.1029/2004GL019929.

[17]Christensen, A. B. et al., "Initial Observations with the Global Ultraviolet Imager (GUVI) in the NASA TIMED Satellite Mission", *J. Geophys. Res*, 108, 2003, doi:10.1029/2003JA009918.

[18]Woods, T.N., F. G. Esparvier, S. M. Bailey, P. C. Chamberlin. J. Lean, G. J. Rottman, S. C. Solomon, W. K. Tobiska and D, L, Woodraska, "Solar EUV Experiment (SEE): Mission Overview and First Results", *J. Geophys. Res.*, 110, AO1312, doi:1029/ 2004JA010765, 2005.

[19]Paxton, L. J. et al., "Special Sensor UV Spectrographic Imager (SSUSI): An Instrument Description", *Instrum. Planet. Terr. Atmos. Remote Sens.*,1745, 1992, p. 2.

[20]Marcos, F. A. J. O. Wise, M. J. Kendra and N. J. Grossbard, "Satellite Drag Research: Past, Present and Future", *Adv. Astronaut. Sci.*, 116, 2004, p. 1865.

[21]Bowman, B. R., F. A. Marcos, and M. J. Kendra, "A Method for Computing Accurate Daily Atmospheric Density Values from Satellite Drag Data", AAS-04-173, *AAS/AIAA Flight Mechanics Meeting*, Maui, HI, 2004.

[22]Keating, G. M., R. H. Tolson and M. S. Bradford,, "Evidence of Long-Term Global Decline in the Earth's Thermospheric Densities Apparently Related to Anthropogenic Effects", *Geophys. Res. Lett.*, 27, 2002, p. 1523.

[23]Emmert, J. T., J. M. Picone, J. L. Lean and S. H. Knowles, "Global Change in the Thermosphere: Compelling Evidence of a Secular Decrease in Density, *J. Geophys. Res.*, 109, 2004, , doi: 10.1029/2003JA010176.

[24]Marcos, F. A. J. O. Wise, M. J. Kendra, N. J. Grossbard and B. R. Bowman, "Detection of a Long-Term Decrease in Thermospheric Neutral Density", *Geophys.Res.Lett.*,32, 2005, doi: 10.1029/ 2004GL021269.

[25]Clilverd, M. A., T. Ulrich and M. J. Jarvis, "Residual Solar Cycle Influence On Trends In Ionospheric F2-Layer Peak Height", *J.Geophys. Res.*,108(A12), 1450, 2003, doi:10.1029/2002JA009896.

[26]Roble, R. G. and R. E. Dickinson, "How Will Changes In Carbon Dioxide And Methane Modify The Mean Structure Of The Mesosphere And Thermosphere?", *Geophys. Res. Lett.*, 16,1989, p. 1441.

[27]S. J. Casali,. W. N. Barker and M. F. Storz, "Dynamic Calibration Atmosphere (DCA) "Tool for the High Accuracy Satellite Drag Model (HASDM)", AIAA 2002-4888, *AAS/AIAA Astrodynamics Specialist Conference*, Monterey, CA, 2002.

[28]B. R. Bowman, "True Satellite Ballistic Coefficient Determination for HASDM", AIAA-2002-4887, *AAS/AIAA Astrodynamics Specialist Conference*, Monterey, CA, 2002.

[29]M. F. Storz, B. R. Bowman and Maj. J. L. Branson, "High Accuracy Satellite Drag Model (HASDM)", AIAA 2002-4886, *AAS/AIAA Astrodynamics Specialist Conference*, , Monterey, CA, 2002.

[30]Bowman, B. R., Tobiska, W. K., and Marcos, F. A., "A New Empirical Thermospheric Density Model JB2006 Using New Solar Indices", AIAA 2006-6166, *AIAA Astrodynamics Conference*, Keystone, CO, Aug. 2006.

[31]Marcos, F. A., B. R. Bowman and R.E. Sheehan, "Statistical Evaluation of the Jacchia-Bowman 2006 Thermospheric Neutral Density Model", AIAA 2006-6166, *AIAA Astrodynamics Conference*, Keystone, CO, Aug. 2006

[32] Lühr, H., M. Rother, W, Koehler, P. Ritter, and L. Grunwaldt, "Thermospheric Up-Welling in the Cusp Region: Evidence from CHAMP Observations", *Geophys. Res. Lett.*, 31, 2004, LO6805, doi:10.1029/2003GL019314.

[33]Demars, H. G. and R. W. Schunk, "Thermospheric Response to Ion Heating in the Dayside Cusp", *J. Atmos and Solar-Terr Res*, In Press.

[34]Fuller-Rowell, T.J., M. Codrescu, and S. Queagan, "On The Seasonal Response Of The Thermosphere And Ionosphere To Geomagnetic Storms", *J. Geophys. Res.*, 101, 1996. p. 2343.

[35]Liu H., H. Lühr, "Strong Disturbance of the Upper Thermospheric Density Due to Magnetic Storms: CHAMP Observations", *J. Geophys. Res.*, 110, 2005, A09S29, doi:10.1029/2004JA010908.

[36]Sutton E. K., J. M. Forbes, R. S. Nerem, "Global Thermospheric Neutral Density And Wind Response To The Severe 2003 Geomagnetic Storms From CHAMP Accelerometer Data", *J. Geophys. Res.*, 110, 2005, A09S40, doi: 10.1029 /2004JA010985.

[37]Marcos , F. A. "New Measurements Of Thermospheric Neutral Density: A Review", AAS 05-251, *AAS/AIAA Astrodynamics Conference*, Lake Tahoe, CA, 2005.

[38]Huang, C.Y., Burke, W.J., "Transient Sheets Of Field-Aligned Current Observed By DMSP During The Main Phase Of A Magnetic Storm", *J. Geophys. Res.*, 109, 2004, A06303 doi: 10.129/2003JA010067.

[39]Burke, W. J., C. Y. Huang, F. A. Marcos and J. O. Wise, "Interplanetary Control Of Thermospheric Densities During Large Magnetic Storms", *J. Atmos Solar-Terr Phys,* 69, 2007, p. 279.

[40]Hedin, A.E. et al., "Revised Global Model of Thermosphere Winds Using Satellite and Ground-Based observations", *J. Geophys. Res.*, 96, 1991, p. 7657.